J. Fluid Mech. (1970), *vol.* 43, *part* 3, *pp.* 477–486
Printed in Great Britain

Periodic boundary layer near a two-dimensional stagnation point

By HIROSHI ISHIGAKI

Rocket Propulsion Division, National Aerospace Laboratory, Tokyo, Japan

(Received 16 January 1970)

The time-mean characteristics of the laminar boundary layer near a two-dimensional stagnation point, when the velocity of the oncoming flow relative to the body oscillates are investigated analytically. First, when the amplitude of the oscillating velocity is small compared with the oncoming flow velocity, a series expansion is made and the obtained equations are solved numerically. The equations are also solved approximately in the extreme cases when the frequency is low and high. The obtained approximate solutions are compared with the numerical solutions in terms of skin friction. Next, when the frequency is high, the finite-velocity-amplitude case is treated. Time-mean velocity profiles and skin friction are obtained and compared with the small-amplitude case.

1. Introduction

Most theoretical investigations concerned with the periodic boundary layers have focused attention on instantaneous behaviour (e.g. fluctuating skin friction). Lighthill (1954) studied the effect of a fluctuating, oncoming stream on the skin friction and heat transfer of a two-dimensional body. Hori (1961) studied flow around an oscillating cylinder for low frequency. Mori & Tokuda (1966) made a theoretical and experimental study of heat transfer from an oscillating cylinder. These investigations considered small amplitude oscillation in which the oscillating velocity amplitude is small compared with the oncoming stream velocity. Lin (1957) considered the effect of finite-amplitude oscillation on a flow field.

As to the time-mean flow field, the only reliable account we have is of the case in which the circular cylinder oscillates in a fluid at rest, first given by Schlichting (1932). In the case when the oncoming stream is present, Lin (1957) made the instructive, qualitative suggestion that the pressure gradient along a body surface plays an important role in the effect of high-frequency oscillation on the time-mean flow field. But we have no quantitative knowledge of the time-mean flow field itself (e.g. of the velocity profile or skin friction).

The principal aim of the present paper is to investigate the time-mean characteristics of the periodic boundary layer near a two-dimensional stagnation point. The particular case of two-dimensional flow about a fixed body, when the fluctuations in the external flow are produced by fluctuations of the oncoming stream, is considered in the following analysis. In an incompressible flow, the

analysis applies also to the case when the fluctuations in relative velocity arise from oscillations of the body parallel to the steady oncoming stream. In general, periodic unsteadiness affects the viscous fluid in the manner of constant thickness (penetration depth). Therefore, when the oscillations are superimposed to the steady stream, flow similarity can no longer be maintained except when the steady boundary-layer thickness is constant. This constant thickness character of stagnation point makes it possible to reduce the unsteady boundary-layer equation to an ordinary differential equation.

2. Small-velocity amplitude case

The boundary-layer equations for two-dimensional unsteady laminar flow of an incompressible fluid are

$$\frac{\partial u}{\partial x}+\frac{\partial v}{\partial y}=0, \tag{1}$$

$$\frac{\partial u}{\partial t}+u\frac{\partial u}{\partial x}+v\frac{\partial u}{\partial y}=\frac{\partial U}{\partial t}+U\frac{\partial U}{\partial x}+\nu\frac{\partial^2 u}{\partial y^2}, \tag{2}$$

$$u=v=0 \text{ at } y=0, \quad u=U(x,t) \quad \text{as} \quad y\to\infty,$$

where x and y are distances parallel and normal to the surface, u and v are the corresponding velocity components, t the time, U the velocity at the edge of the boundary layer, and ν the kinematic viscosity. Near a front stagnation point, the velocity $U(x,t)$ is assumed to be

$$U(x,t)=Ax(1+\epsilon e^{i\omega t}), \tag{3}$$

where A is constant and ω is frequency.

When ϵ is small compared with unity, u and v may be expanded as

$$\left.\begin{aligned} u(x,y,t) &= u_0(x,y)+\epsilon u_1(x,y,t)+\epsilon^2 u_2(x,y,t)+\ldots,\\ v(x,y,t) &= v_0(x,y)+\epsilon v_1(x,y,t)+\epsilon^2 v_2(x,y,t)+\ldots. \end{aligned}\right\} \tag{4}$$

Substituting the (4) into (1) and (2), and equating the same order of ϵ, sets of equations are obtained. The zeroth-order equations are

$$\frac{\partial u_0}{\partial x}+\frac{\partial v_0}{\partial y}=0, \tag{5a}$$

$$u_0\frac{\partial u_0}{\partial x}+v_0\frac{\partial v_0}{\partial y}=A^2x+\nu\frac{\partial^2 u_0}{\partial y^2}, \tag{5b}$$

$$u_0=v_0=0 \quad \text{at} \quad y=0, \quad u_0=Ax \quad \text{as} \quad y\to\infty.$$

The solutions are the following well-known functions:

$$u_0=Axf'(\eta), \quad v_0=-\sqrt{(A\nu)}f(\eta), \quad \eta=y\sqrt{(A/\nu)}, \tag{6}$$

where prime denotes differentiation with respect to η. The first-order equations are

$$\frac{\partial u_1}{\partial x}+\frac{\partial v_1}{\partial y}=0, \tag{7a}$$

$$\frac{\partial u_1}{\partial t}+u_0\frac{\partial u_1}{\partial x}+u_1\frac{\partial u_0}{\partial x}+v_0\frac{\partial u_1}{\partial y}+v_1\frac{\partial u_0}{\partial y}=(i\omega+2A)Ax\,e^{i\omega t}+\nu\frac{\partial^2 u_1}{\partial y^2}, \tag{7b}$$

$$u_1=v_1=0 \quad \text{at} \quad y=0, \quad u_1=Ax\,e^{i\omega t} \quad \text{as} \quad y\to\infty.$$

By analogy with (6), solutions are assumed to be

$$u_1 = Axg'(\eta)e^{i\omega t}, \quad v_1 = -\sqrt{(A\nu)}g(\eta)e^{i\omega t}. \tag{8}$$

Substitutions of (8) into (7) yield the following ordinary differential equation:

$$\left.\begin{aligned} &g''' + fg' - 2f'g' + f''g - \frac{i\omega}{A}g' = -\frac{i\omega}{A} - 2, \\ &g = g' = 0 \quad \text{at} \quad \eta = 0, \quad g' = 1 \quad \text{as} \quad \eta \to \infty. \end{aligned}\right\} \tag{9}$$

Since (9) contains the frequency parameter $\sigma = \omega/A$, approximate solutions have been sought in the extreme cases when the frequency parameter is small and large. When σ is smaller than unity, the following power series solution is obtained (Hori 1961):

$$g(\eta) = g_0(\eta) + i\sigma g_1(\eta) + (i\sigma)^2 g_2(\eta) + \ldots. \tag{10}$$

When σ is larger than unity, Mori & Tokuda have obtained the following solution by WKB method:

$$\left.\begin{aligned} &g(\eta) = \left(\eta - \frac{1}{\sqrt{(i\sigma)}} + \ldots\right) + \left(\frac{1}{\sqrt{(i\sigma)}} + \ldots\right)e^{\xi(\eta)}, \\ &\xi(\eta) = -\sqrt{(i\sigma)}\left(\eta + \frac{1}{2\sqrt{(i\sigma)}}\int_0^\eta f\,d\eta + \ldots\right). \end{aligned}\right\} \tag{11}$$

Here, numerical solutions are obtained for given values of σ and compared with the former approximate solutions in terms of skin friction. From (10) and (11), the following expressions are obtained:

$$\frac{\tau_{wt}}{\tau_{w0}} = \tfrac{3}{2} + 0{\cdot}225i\sigma - 0{\cdot}020(i\sigma)^2 + \ldots \quad \text{(small } \sigma\text{)}, \tag{12a}$$

$$= 0{\cdot}8113\sqrt{(i\sigma)} + \frac{1{\cdot}623}{\sqrt{(i\sigma)}} - \frac{0{\cdot}875}{i\sigma} + \ldots \quad \text{(large } \sigma\text{)}, \tag{12b}$$

where

$$\tau_{w0} = \mu\left(\frac{\partial u_0}{\partial y}\right)_{y=0}, \quad \tau_{wt} = \mu\left(\frac{\partial u_1}{\partial y}\right)_{y=0},$$

μ being the viscosity. The amplitude and phase angle of fluctuating skin friction of order ϵ obtained numerically are shown in figure 1 by solid lines, as well as the approximate results (12*a*) and (12*b*), which are shown by dotted lines. It may be said that the agreement is fairly good. The asymptotic values obtained by Lighthill are also shown by broken lines, and we can see that the asymptotic phase advance 45° may be attained at very large value of σ.

The second-order equations are

$$\frac{\partial u_2}{\partial x} + \frac{\partial v_2}{\partial y} = 0, \tag{13a}$$

$$\frac{\partial u_2}{\partial t} + u_0\frac{\partial u_2}{\partial x} + u_1\frac{\partial u_1}{\partial x} + u_2\frac{\partial u_0}{\partial x} + v_0\frac{\partial u_2}{\partial y} + v_1\frac{\partial u_1}{\partial y} + v_2\frac{\partial u_0}{\partial y} = \tfrac{1}{2}A^2x(1 + e^{2i\omega t}) + \nu\frac{\partial^2 u_2}{\partial y_2}, \tag{13b}$$

$$u_2 = v_2 = 0 \quad \text{at} \quad y = 0, \quad u_2 = 0 \quad \text{as} \quad y \to \infty.$$

Solutions may be represented as

$$u_2 = Ax\{G'(\eta) + G'_a(\eta)\, e^{2i\omega t}\}, \quad v_2 = -\sqrt{(A\nu)}\,\{G(\eta) + G_a(\eta)\, e^{2i\omega t}\}. \tag{14}$$

Then the time-independent function G satisfies the following ordinary differential equation

$$G''' + fG'' - 2f'G' + f''G = \tfrac{1}{2}\{g_r'^2 + g_i'^2 - g_r g_r'' - g_i g_i'' - 1\}, \tag{15}$$

$$G = G' = 0 \quad \text{at} \quad \eta = 0, \quad G' = 0 \quad \text{as} \quad \eta \to \infty,$$

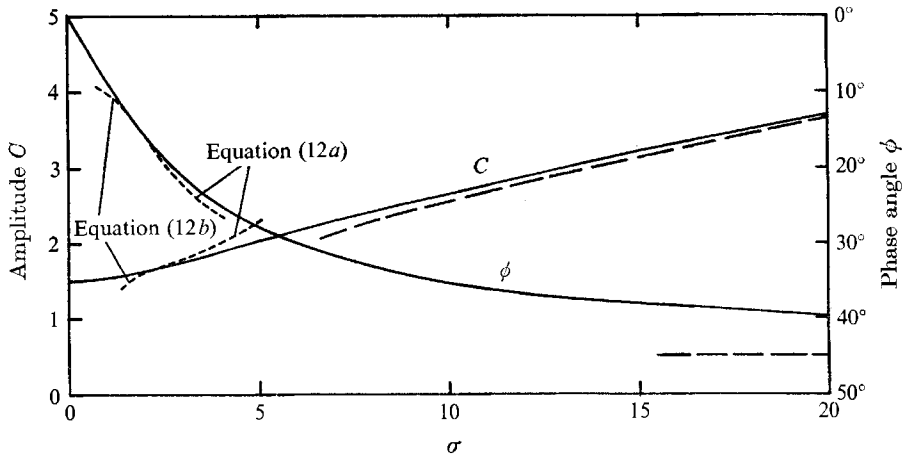

FIGURE 1. Amplitude and phase angle of fluctuating component of skin friction.

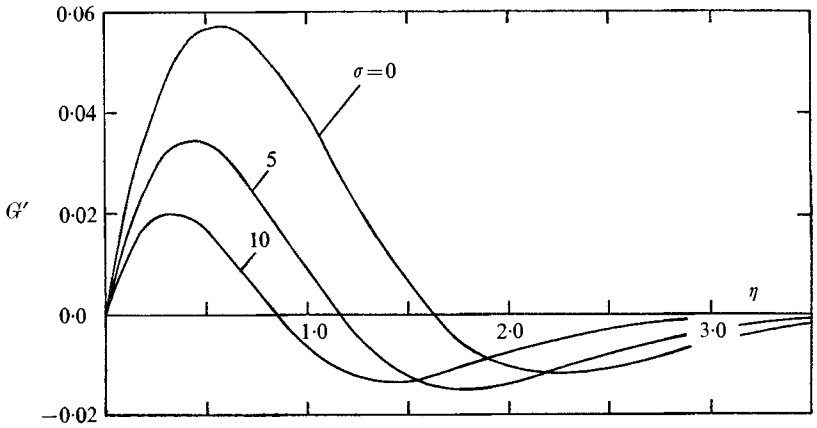

FIGURE 2. Plot of the function G'.

where subscript r and i respectively denote real and imaginary part of each function. Numerical solutions are obtained using the solutions of (9) in the right-hand side of (15). Some typical functions G', which are proportional to the time-mean deviation from the steady velocity profile caused by flow oscillation, are shown in figure 2. It can be seen that the fluid near a wall is accelerated, and that the magnitude of this acceleration is larger for smaller values of σ.

For comparison, and so as to see the characteristics in analytical form,

approximate solutions are also obtained in the following manner. For small σ, the power series solution may be assumed to be

$$G(\eta) = G_0(\eta) + \sigma G_1(\eta) + \sigma^2 G_2(\eta) + \ldots. \tag{16}$$

Substituting (10) and (16) into (15), and equating the same order of σ, the following equations are obtained:

$$\left.\begin{aligned} &G_0''' + fG_0'' - 2f'G_0' + f''G_0 = \tfrac{1}{2}\{g_0'^2 - g_0 g_0'' - 1\}, \\ &G_1''' + fG_1'' - 2f'G_1' + f''G_1 = 0, \\ &G_2''' + fG_2'' - 2f'G' + f''G_2 = \tfrac{1}{2}\{g_1'^2 - 2g_0'g_2' + g_0''g_2 - g_1g_1'' + g_0g_2''\}, \end{aligned}\right\} \tag{17}$$

$$G_0 = G_0' = G_1 = G_1' = G_2 = G_2' = 0 \quad \text{at} \quad \eta = 0,$$

$$G_0' = G_1' = G_2' = 0 \quad \text{as} \quad \eta \to \infty.$$

Here G_0 is the quasi-steady-state solution, G_1 is identically zero and G_2 is obtained numerically, giving

$$G_0 = \tfrac{1}{16}(-f + \eta f' + \eta^2 f''), \quad G_1 = 0, \quad G_2''(0) = -0{\cdot}004.$$

For large σ, substitution of (11) into the right-hand side of (15) yields

$$G''' + fG'' - 2f'G' + f''G = \frac{f''}{2\sigma\sqrt{(2\sigma)}} + \ldots + \{-\tfrac{1}{4}\eta\sqrt{(2\sigma)} - 1 - \tfrac{1}{2}\eta f + \ldots\}\cos\xi_i e^{\xi r} + \{\tfrac{1}{4}\eta\sqrt{(2\sigma)} - \tfrac{1}{2} + \ldots\}\sin\xi_i e^{\xi r} + \{\tfrac{1}{2} + \ldots\}e^{2\xi r}. \tag{18}$$

Then the solution in the following form may be assumed:

$$G(\eta) = G_b(\eta) + G_c(\eta)\cos\xi_i e^{\xi r} + G_d(\eta)\sin\xi_i . e^{\xi r} + G_e(\eta)\, e^{2\xi r}. \tag{19}$$

Since the terms in (19) are linearly independent, equations for G_b, G_c, G_d and G_e are obtained after substituting (19) into (18). Solutions of these equations are

$$G_c = \frac{1}{\sigma\sqrt{(2\sigma)}}\{-3 - \tfrac{1}{4}\eta f) + \ldots\}, \quad G_d = \frac{1}{\sigma}\left\{\tfrac{1}{2}\eta + \frac{1}{\sqrt{(2\sigma)}}(2 + \tfrac{1}{4}\eta f) + \ldots\right\},$$

$$G_e = \frac{1}{\sigma\sqrt{(2\sigma)}}\{-\tfrac{1}{4} + \ldots\}.$$

It is readily understood that the following conditions are to be attached to G_b so as to satisfy the boundary conditions,

$$G_b(0) = \frac{1}{\sigma\sqrt{(2\sigma)}}(\tfrac{13}{4}) + O\left(\frac{1}{\sigma^3}\right), \quad G_b'(0) = \frac{1}{\sigma}(-\tfrac{3}{4}) + O\left(\frac{1}{\sigma^2\sqrt{\sigma}}\right).$$

Therefore, expressing

$$G_b(\eta) = \frac{1}{\sigma}\left\{G_{b0}(\eta) + \frac{1}{\sqrt{(2\sigma)}}G_{b1}(\eta) + \ldots\right\},$$

the following equations are obtained for each order of σ:

$$G_{b0}''' + fG_{b0}'' - 2f'G_{b0}' + f''G_{b0} = 0,$$

$$G_{b1}''' + fG_{b1}'' - 2f'G_{b1}' + f''G_{b1} = \tfrac{1}{2}f'',$$

$$G_{b0} = 0, \quad G_{b0}' = -\tfrac{3}{4}, \quad G_{b1} = \tfrac{13}{4}, \quad G_{b1}' = 0 \quad \text{at} \quad \eta = 0,$$

$$G_{b0}' = G_{b1}' = 0 \quad \text{as} \quad \eta \to \infty.$$

Numerical calculations give

$$G''_{b0}(0) = 0{\cdot}608, \quad G''_{b1}(0) = 1{\cdot}449.$$

These approximate sclutions give the following time-mean skin friction:

$$\frac{\bar{\tau}_w}{\tau_{w0}} = 1+\epsilon^2 T(\sigma),$$

$$T(\sigma) = \tfrac{3}{16} - 0{\cdot}0033\sigma^2 + \ldots \quad \text{(small } \sigma\text{)}, \tag{20a}$$

$$= \frac{0{\cdot}2868}{\sqrt{\sigma}} + \frac{0{\cdot}4932}{\sigma} + \frac{0{\cdot}8313}{\sigma\sqrt{\sigma}} + \ldots \quad \text{(large } \sigma\text{)}, \tag{20b}$$

where

$$\bar{\tau}_w = \frac{1}{2\pi}\int_0^{2\pi} \mu \left(\frac{\partial u}{\partial y}\right)_{y=0} dt.$$

Numerical results are shown in figure 3 by a solid line, and the approximate results (20*a*) and (20*b*) by a dotted line. Many more terms in (20*b*) will be required for better agreement. The asymptotic value for very large σ, first term only in

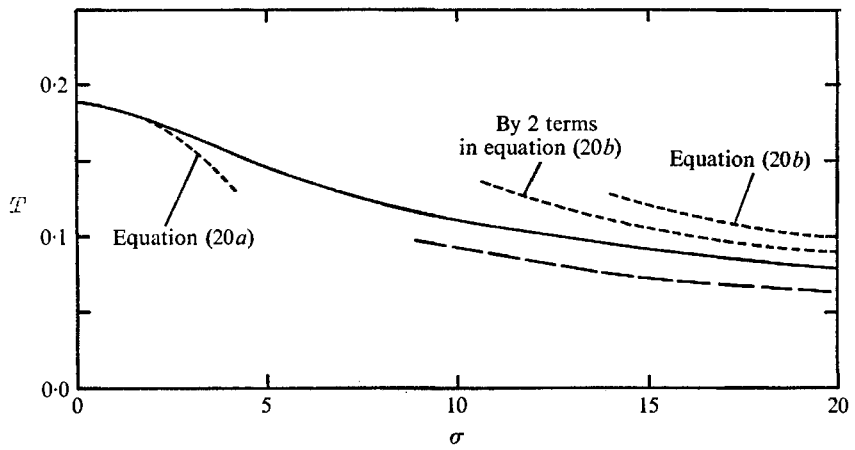

FIGURE 3. Plot of T with frequency parameter σ.

(20*b*), is also shown by a broken line. It can be seen that the first term in (20*b*) results from the acoustic streaming near the wall in the absence of an oncoming stream. Therefore the difference between the solid line and the broken line gives roughly the contribution of the oncoming stream. In this analysis, acoustic streaming outside the boundary layer is neglected, and it is discussed only briefly in §3.

3. Finite-velocity amplitude case

The basic equations in the boundary layer are identical with those of §2, i.e. (1) and (2). The main-stream velocity outside the boundary layer is given by (3) without retriction on ϵ.

Following Lin, the velocity in the boundary layer may be separated into two components (time-mean and fluctuating):

$$\left.\begin{aligned} u(x,y,t) &= \bar{u}(x,y)+u_t(x,y,t)\\ v(x,y,t) &= \bar{v}(x,y)+v_t(x,y,t),\\ \bar{u}_t &= \bar{v}_t = 0, \end{aligned}\right\} \tag{21}$$

where the bar over a symbol denotes time-mean quantities. Substituting (21) into (1) and (2), and taking its time average, the following time-mean equations are obtained:

$$\frac{\partial \bar{u}}{\partial x}+\frac{\partial \bar{v}}{\partial y} = 0, \tag{22a}$$

$$\bar{u}\frac{\partial \bar{u}}{\partial x}+\bar{v}\frac{\partial \bar{u}}{\partial y} = A^2x\left(1+\frac{\epsilon^2}{2}\right)-\overline{u_t\frac{\partial u_t}{\partial x}}-\overline{v_t\frac{\partial u_t}{\partial y}}+\nu\frac{\partial^2\bar{u}}{\partial y^2}, \tag{22b}$$

$$\bar{u}=\bar{v}=0 \quad \text{at} \quad y=0, \quad \bar{u}=Ax \quad \text{as} \quad y\to\infty.$$

Subtracting (22*a*) and (22*b*) from the full equations (1) and (2) respectively, the following fluctuating equations are obtained:

$$\frac{\partial u_t}{\partial x}+\frac{\partial v_t}{\partial y} = 0, \tag{23a}$$

$$\frac{\partial u_t}{\partial t}+\bar{u}\frac{\partial u_t}{\partial x}+u_t\frac{\partial \bar{u}}{\partial x}+u_t\frac{\partial u_t}{\partial x}-\overline{u_t\frac{\partial u_t}{\partial x}}+\bar{v}\frac{\partial u_t}{\partial y}+v_t\frac{\partial \bar{u}}{\partial y}+v_t\frac{\partial u_t}{\partial y}-\overline{v_t\frac{\partial u_t}{\partial y}}$$
$$= \epsilon Ax(i\omega+2A)e^{i\omega t}+\frac{\epsilon^2}{2}A^2xe^{2i\omega t}+\nu\frac{\partial^2 u_t}{\partial y^2}, \tag{23b}$$

$$u_t=v_t=0 \quad \text{at} \quad u=0, \quad u_t=\epsilon Axe^{i\omega t} \quad \text{as} \quad y\to\infty.$$

In the case of high frequency, the following assumptions are made:

$$\frac{\partial u_1}{\partial t}\gg \bar{u}\frac{\partial u_t}{\partial x}, \quad \frac{\partial u_1}{\partial t}\gg u_t\frac{\partial u_t}{\partial x}, \quad \text{or} \quad \sigma\gg 1, \quad \sigma\gg\epsilon. \tag{24a}$$

Then (23*b*) is simplified to

$$\frac{\partial u_t}{\partial t} = i\omega\epsilon Axe^{i\omega t}+\nu\frac{\partial^2 u_t}{\partial y^2}. \tag{24}$$

The solutions of (23*a*) and (24) obtained by Lin were

$$\left.\begin{aligned} u_t &= \epsilon Ax\{1-\exp(-\sqrt{(i\omega/\nu)}\,y)\}e^{i\omega t},\\ v_t &= -\epsilon A\sqrt{(\nu/i\omega)}\{\sqrt{(i\omega/\nu)}\,y-1+\exp(-\sqrt{(i\omega/\nu)}\,y)\}e^{i\omega t}. \end{aligned}\right\} \tag{25}$$

The additional terms in (22*b*) can be estimated as

$$\begin{aligned} P(x,y) &\equiv \frac{\epsilon^2}{2}A^2x-\overline{u_t\frac{\partial u_t}{\partial x}}-\overline{v_t\frac{\partial u_t}{\partial y}},\\ &= \frac{\epsilon^2}{2}A^2x\left\{\left(\frac{y}{\delta_0}+2\right)\cos\frac{y}{\delta_0}+\left(\frac{y}{\delta_0}-1\right)\sin\frac{y}{\delta_0}-\exp\left(-\frac{y}{\delta_0}\right)\right\}\exp\left(-\frac{y}{\delta_0}\right),\\ &\equiv \frac{\epsilon^2}{2}A^2xP_1\left(\frac{y}{\delta_0}\right), \end{aligned} \tag{26}$$

where $\delta_0=\sqrt{(2\nu/\omega)}$ is the so-called penetration depth or viscous wave thickness.

The time-mean flow equations are now rewritten as

$$\frac{\partial \overline{u}}{\partial x}+\frac{\partial \overline{v}}{\partial y}=0, \tag{27a}$$

$$\overline{u}\frac{\partial \overline{u}}{\partial x}+\overline{v}\frac{\partial \overline{u}}{\partial y}=A^2x\{1+\tfrac{1}{2}\epsilon^2P_1\}+\nu\frac{\partial^2\overline{u}}{\partial y^2}. \tag{27b}$$

The following transformations are made:

$$\overline{u}=AxF'(\eta),\quad \overline{v}=-\sqrt{(A\nu)}\,F(\eta). \tag{28}$$

Then a non-linear ordinary differential equation including two parameters, ϵ and σ, is obtained:

$$F'''+FF''-F'^2+1+\tfrac{1}{2}\epsilon^2P_1(\sqrt{(\tfrac{1}{2}\sigma)}\,\eta)=0, \tag{29}$$
$$F=F'=0 \quad \text{at} \quad \eta=0, \quad F'=1 \quad \text{as} \quad \eta\to\infty.$$

Solutions are obtained numerically for given values of ϵ and σ. Initial values of these solutions $F''(0)$ are shown in table 1, as well as per cent differences referred

$\sigma = 10$		$\sigma = 20$		$\epsilon = 2{\cdot}0$	
ϵ	$F''(0)$	ϵ	$F''(0)$	σ	$F''(0)$
0·5	1·2678 (0·06 %)	0·5	1·2570 (0·01 %)	3	2·1403 (4·81 %)
1·0	1·4248 (0·20 %)	1·0	1·3301 (0·02 %)	5	1·9901 (2·14 %)
1·5	1·5482 (0·33 %)	1·5	1·4518 (0·02 %)	7	1·8915 (1·06 %)
2·0	1·7915 (0·40 %)	2·0	1·6217 (−0·01 %)	10	1·7915 (0·40 %)
3·0	2·4767 (0·11 %)	3·0	2·1038 (−0·02 %)	13	1·7228 (0·15 %)
4·0	3·4119 (−0·80 %)	4·0	2·7706 (−0·07 %)	15	1·6875 (0·06 %)

TABLE 1. Initial values of function $F''(\eta)$ at various values of ϵ and σ. (Differences from the extrapolated values of small amplitude case shown in parentheses)

to the extrapolated values of the small amplitude case. From this it is anticipated that small amplitude solutions give the well-approximated values for large σ, even if the amplitude grows finite. Figures 4 and 5 show some typical velocity profiles F' in solid lines, and additional pressure gradient P_1 in broken lines. It can be seen that, when σ is large, influences of additional pressure gradient are restricted to the immediate neighbourhood of the wall and neutralized by intense viscous force. As σ becomes smaller, the additional pressure gradient influences the intermediate region of weak viscous force and accelerates the fluid there. This seems a reasonable explanation of the physical dependency of time-mean skin friction on σ.

Finally, we consider the condition of negligible secondary flow velocity outside the boundary layer. Secondary flow far from the wall may be expected to have an appreciable effect when the velocity amplitude grows finite. A rough criterion

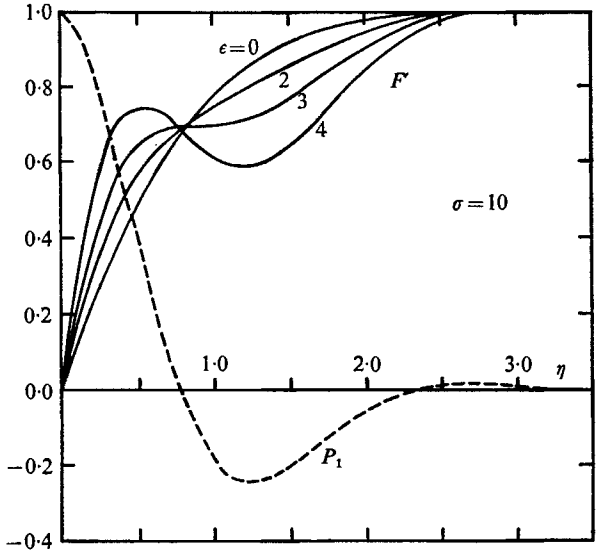

FIGURE 4. Time-mean velocity profile F' and additional pressure gradient P_1 when $\sigma = 10{\cdot}0$.

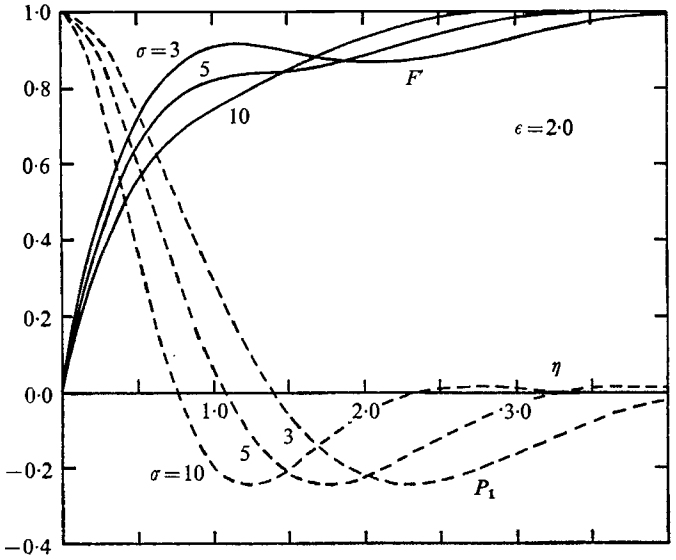

FIGURE 5. Time-mean velocity profile F' and additional pressure gradient P_1 when $\epsilon = 2{\cdot}0$.

we can use is derived from the secondary flow without the steady oncoming stream. According to Schlichting, it is of the order of $(\epsilon^2 A^2 x)/\omega$, and we can see that this becomes negligible in the time-mean pressure gradient and outer boundary condition when the following inequality is added to the above-mentioned inequalities (24*a*):

$$\sigma \gg \epsilon^2. \tag{24b}$$

This work was performed at Institute of High Speed Mechanics, Tohoku University, and the author would like to acknowledge the continuing guidance and encouragement of Professor T. Yuge.

REFERENCES

HORI, E. 1961 *Trans. Japan Soc. Mech. Engng,* **27**, 167.
LIGHTHILL, M. J. 1954 *Proc. Roy. Soc.* A **224**, 1.
LIN, C. C. 1957 *Proc. 9th Int. Cong. Appl. Mech.* **4**, 155.
MORI, Y. & TOKUDA, S. 1966 *Proc. 3rd Int. Heat Transfer Conf.* **3**, 49.
SCHLICHTING, H. 1932 *Phys. Z.* **33**, 97.